SARS-CoV-2 exposure in Norway rats (*Rattus norvegicus)* from New York City

Yang Wang[1,2,3], Julianna Lenoch[4], Dennis Kohler[4], Thomas J. DeLiberto[5*], Cynthia Tang[1], Tao Li[6], Yizhi Jane Tao[7], Minhui Guan[1,2,3], Susan Compton[8], Caroline Zeiss[8], Jun Hang[6], and Xiu-Feng Wan[1,2,3,9,*]

[1]Center for Influenza and Emerging Infectious Diseases, University of Missouri, Columbia, Missouri, USA; [2]Department of Molecular Microbiology and Immunology, School of Medicine, University of Missouri, Columbia, Missouri, USA; [3]Bond Life Sciences Center, University of Missouri, Columbia, Missouri, USA; [4]USDA APHIS Wildlife Services National Wildlife Disease Program, Fort Collins, Colorado, USA; [5]USDA APHIS Wildlife Services, Fort Collins, Colorado, USA; [6]Viral Diseases Branch, Walter Reed Army Institute of Research, Silver Spring, Maryland, USA; [7]Department of BioSciences, Rice University, Houston, TX, USA; [8]School of Medicine, Yale University, New Haven, Connecticut, USA; [9]Department of Electrical Engineering & Computer Science, College of Engineering, University of Missouri, Columbia, Missouri, USA.

* Xiu-Feng Wan; Thomas J. DeLiberto

Email: wanx@missouri.edu; thomas.j.deLiberto@usda.gov

Author Contributions: XFW, JL, DK, and TD conceived the experiments. XFW, JL, DK, TD, and YW designed the experiments. JL, DK, and TD contributed to the wild rat capture. YW, TL, JT, and MG performed the experiments. SC and CZ provided study materials. YW, CT, JT, TL, and JH analyzed the data. YW and XFW prepared the original draft. All authors did substantial contribution to revision of this paper.

Competing Interest Statement: The authors have declared that no competing interests exist.

Keywords: SARS-CoV-2, rat, surveillance, infection

This file includes:

> Main Text
> Figures 1 to 4
> Tables 1
> Table S1-S3

Abstract

Millions of Norway rats (*Rattus norvegicus*) inhabit New York City (NYC), presenting the potential for transmission of SARS-CoV-2 from humans to rats and other wildlife. We evaluated SARS-CoV-2 exposure among 79 rats captured from NYC during the fall of 2021. Results showed that 13 of 79 rats (16.5%) tested IgG or IgM positive, and partial genomes of SARS-CoV-2 were recovered from four rats that were qRT-PCR positive. Using a virus challenge study, we also showed that Alpha, Delta, and Omicron variants can cause robust infections in wild-type Sprague Dawley (SD) rats, including high level replications in the upper and lower respiratory tracts and induction of both innate and adaptive immune responses. Additionally, the Delta variant resulted in the highest infectivity. In summary, our results indicated that rats are susceptible to infection with Alpha, Delta, and Omicron variants, and rats in the NYC municipal sewer systems have been exposed to SARS-CoV-2. Our findings highlight the potential risk of secondary zoonotic transmission from urban rats and the need for further monitoring of SARS-CoV-2 in those populations.

Importance

Since its emergence causing the COVID-19 pandemic, the host tropism expansion of SARS-CoV-2 raises a potential risk for reverse-zoonotic transmission of emerging variants into rodent species, including wild rat species. In this study, we presented both genetic and serological evidence for SARS-CoV-2 exposure in wild rat population from New York City, and these viruses are potentially linked to the viruses during the early stages of the pandemic. We also demonstrated that rats are susceptible to additional variants (i.e., Alpha, Delta, and Omicron) predominant in humans and that the susceptibility to different variants vary. Our findings highlight the potential risk of secondary zoonotic transmission from urban rats and the need for further monitoring of SARS-CoV-2 in those populations.

Introduction

As of October 10, 2022, severe acute respiratory syndrome coronavirus 2 (SARS-CoV-2), the virus responsible for coronavirus disease 2019 (COVID-19), has caused approximately 621 million human cases and 6.6 million deaths globally (1). In addition to humans, a wide range of wild, domestic, and captive animals were documented with exposure to SARS-CoV-2, such as deer, mink, otters, ferrets, hamsters, gorillas, cats, dogs, lions, and tigers (2-4). SARS-CoV-2 in farmed mink was shown to cause infections in humans (5), highlighting mink as a potential reservoir for secondary zoonotic infections.

SARS-CoV-2 has undergone rapid evolution, and a large number of genetic variants have been identified, including several variants of concern (VOC), such as Alpha (B.1.1.7 lineage), Beta (B.1.351 lineage), Gamma (P.1 lineage), Delta (B.1.617.2 and AY sublineages) and Omicron (B.1.1.529 and BA sublineages). The Alpha, Beta, and Gamma variants were reported to have acquired substitutions at the receptor-binding domain (RBD) of the spike protein that allowed for infectivity in mice and/or rats (6-9). The tropism expansion of SARS-CoV-2 raises a potential risk for reverse-zoonotic transmission of emerging variants into rodent species, including wild mouse and rat species (10). Two independent SARS-CoV-2 serosurveillance studies among wild rats from sewage systems in Belgium (late fall of 2020) and Hong Kong (spring of 2021) suggested possible exposure of these animals to SARS-CoV-2, but no viral RNA was detected (11, 12). With new SARS-CoV-2 variants continuing to emerge, it is still unknown whether the more recent variants of concern (e.g., Delta and Omicron) are infectious to rats.

In this study, we evaluated the capability of Delta and Omicron variants to infect rats (*Rattus norvegicus*) and investigated the exposure of rats to SARS-CoV-2 in New York City (NYC), New York, United Sates.

Results

Detecting SARS-CoV-2 virus in NYC rats.
To evaluate whether wild rats have been exposed to SARS-CoV-2, we conducted SARS-CoV-2 surveillance in Norway rats (*Rattus norvegicus*) in NYC from September 13-November 16, 2021, when the Delta variant was predominant in humans. A total of 79 rats inhabiting three sampling sites in Brooklyn, NYC were captured and sampled. Using ELISA, we identified 9 out of 79 (11.4%) IgG-positive rat serum samples and 4 IgM-positive samples (5.1%) against both Wuhan-Hu-1 spike protein and RBD (Table 1). All 13 seropositive samples were subjected to microneutralization assays against the B.1 lineage and the Alpha and Delta variants. However, all samples were negative for neutralizing antibodies. As a negative control, we used ELISA to examine 9 negative serum samples from uninfected SD rats and 6 serum samples from SD rats infected with rat coronaviruses, Sialodacryoadenitis Virus or Parker's Rat Coronavirus (13); none exhibited IgG or IgM positivity against either spike protein or RBD (Data not shown).

Of all the tissues analyzed from the 79 rats, only four lung samples were positive by qRT-PCR against both N1 and N2 primers using the CDC SARS-CoV-2 diagnostic panel (Table 1). The control group with RNA from 6 different strains of rat coronaviruses remained negative. It is noteworthy that two out of these four rats (Rat #2 and #19) were both seropositive and viral RNA-positive. In addition, we had seven inconclusive samples which were tested positive on either N1 or N2 primer but not both. However, viruses failed to be recovered from Vero E6, 293FT/hACE2+TMPRSS, rat lung epithelial (L2), or rat lung tracheal epithelial cell lines.

After subjecting these four qRT-PCR-positive samples to SARS-CoV-2 genome sequencing, partial SARS-CoV-2 genome was identified in all samples with a viral genome coverage of 1.6% to 21.3% (Table S1). Both molecular characterization and phylogenetic analyses on these partial genomes

82   suggested that viruses in these rats are associated with genetic lineage B, which was predominant
83   in NYC in the spring of 2020 during the early pandemic period (Fig. 1).
84
85   In addition, we subjected these four qRT-PCR-positive and two additional inconclusive samples to
86   pan-viral target hybridization enrichment sequencing. Presence of SARS-CoV-2 sequences were
87   found in three out of four sequenced qRT-PCR-positive samples (Rats# 2, 19, and 43) and one of
88   two inconclusive samples (Rat# 38). No sequence data was obtained for the qRT-PCR-positive
89   sample from Rat# 46. Of interest, rat coronavirus was detected in another inconclusive sample
90   (Rat# 30) (Table S2). The identified SARS-CoV-2 or rat coronavirus reads aligned with a number
91   of genes across the genomes.
92
93   ***Rats displayed varying susceptibility to SARS-CoV-2 variants.***
94   The Alpha variant emerged in late 2020 and quickly became a dominant SARS-CoV-2 variant in
95   NYC; subsequently, the Delta and Omicron variants predominated in NYC starting in June 2021
96   and December 2021, respectively (Fig. 1A). To investigate whether these SARS-CoV-2 variants
97   are capable of infecting rats, we intranasally challenged 6-week-old wild-type SD rats with Alpha,
98   Delta, or Omicron variants and collected tissues at 2- and 4-days post-infection (dpi) (Fig. 2B).
99   Compared to the Wuhan-Hu-1 strain, the Omicron variant used in the challenge study possesses
100 the same N501Y substitution as the Alpha variant and 16 additional substitutions, whereas the
101 Delta variant does not possess N501Y, but contains the L452R and T478K substitutions (Fig. 2C).
102
103 At 2 and 4 dpi, high levels of viral RNA were detected in both turbinate and lungs, and infectious
104 viral titers were detected in turbinate and/or lungs, although no body weight loss or other clinical
105 signs were observed in the rats with any of the variants (Fig. 2D-F). In particular, the lungs from
106 the rats infected with the Delta variant showed both the highest RNA copies and the highest
107 infectious viral titers at 2 dpi (RNA copies: p=0.0081 and 0.0060 for Delta vs. Alpha and Delta vs.
108 Omicron, respectively; infectious viral titers: p=0.0287 and 0.0283 for Delta vs. Alpha and Delta vs.
109 Omicron, respectively). In addition, antigen expression was detected in the lungs of all rats infected
110 with any variant at 2 or 4 dpi (Fig. 2F). In line with the viral titers, the rats infected with the Delta
111 variant showed the highest antigen expression in the lungs compared to those infected with other
112 variants (Fig. 2G).
113
114 To assess the innate and adaptive immune response induced by the virus infection in rats, we
115 determined the cytokine/chemokine expression in the lungs at 2 and 4 dpi and the antibody titers
116 at 21 dpi. The results showed that all infections induced pro-inflammatory cytokine/chemokine
117 expression (i.e., IFN-β, IFN-γ, TNF-α, IL-1α, IL-1β, IL-6, CCL-2, IP-10, IL-10) particularly at 2 dpi
118 (Fig. 3A). The expression of all the cytokines/chemokines induced by the Delta variant was higher
119 than those induced by Alpha and/or Omicron variants.
120
121 Regarding the adaptive immune response, both IgG antibodies and neutralizing antibodies were
122 detected for all three variants at 21 dpi; however, IgM antibodies were not detected in any rats
123 regardless of the variant used (Figures 3B and 3C). There was no significant difference between
124 Alpha and Delta variants in the IgG antibody titers against Wuhan-Hu-1 spike protein or RBD.
125 However, Delta showed significantly higher anti-RBD IgG titers than Omicron. The homologous
126 neutralizing antibody titers induced by the Delta variant were significantly higher than those induced
127 by Alpha or Omicron (p=0.0441 and 0.0040, respectively). These results indicated that all the three
128 variants can infect SD rats and induce innate and adaptive immune responses, and among these
129 three variants, the Delta variant replicates more efficiently than the Alpha and Omicron variants in
130 rats.
131
132 To detect potential host-adapted mutations, we sequenced the lung tissues from the rats
133 challenged with Alpha, Delta, and Omicron. Results suggested there were no adapted amino acid
134 substitutions along the RBDs across the three testing variants. However, N74K (N-terminal domain)
135 on the spike protein was observed in all animals challenged by Alpha, and P681R (SD1/2) and

136 D950N (heptapeptide repeat sequence 1) of spike in all animals challenged by Delta (Table S2). In
137 addition, additional amino acid substitutions in non-structural proteins NSP6, NSP13, and
138 nucleoprotein were observed in some animals challenged by Alpha or Delta. Of interest, no
139 adapted mutations were observed in the animals challenged by Omicron.
140
141 ***Structural modeling between RBD of SARS-CoV-2 variants and rat, mouse, and human***
142 ***ACE2.***
143 To explain the relative replication efficiency of the three SARS-CoV-2 viruses in SD rats, we
144 computationally modeled the interaction between rat ACE2 and RBD from Alpha, Delta and
145 Omicron variants (Fig. 4), as virus-receptor interaction is often an important virulence determinant.
146 In our structural models, residue 452 does not directly engage with rat ACE2, but it is surrounded
147 by a large number of residues nearby (Fig. 4C). Therefore, the L452R mutation in the Delta variant
148 could alter the structure conformation of the adjacent β-strand at the ACE2 interface and thus
149 indirectly modulate ACE2 binding affinity (Fig. 4C). Indeed, in vitro binding assays indicated that
150 the RBD of the Delta variant, which has L452R/T478K double mutations, binds rat ACE2 with a >2-
151 fold stronger affinity than RBD of the prototype virus (14). The enhanced binding of the Delta RBD
152 to rat ACE2 is likely due to L452 alone, because residue 478 is distant from other amino acids, and
153 T478K was found to have no significant effect on binding to mouse ACE2, which is a close homolog
154 of rat ACE2 (15). The Alpha variant also replicates well in rats but is slightly less efficient than Delta.
155 Our structure model shows that the single mutation N501Y in Alpha RBD makes a favorable
156 interaction with H353 in the rat ACE2, with the aromatic side chain of Y501 stacked against the
157 side chain of H453 (Fig. 4D). In vitro binding assays confirmed that the Alpha RBD binds rat ACE2
158 with a >2-fold stronger affinity than RBD of the prototype virus (14), consistent with our structural
159 analysis.
160
161 The Omicron variant has many mutations in its RBD compared to the prototype virus (Fig. 2C).
162 Among these mutations, eight are located near the ACE2 binding interface, including residues 405,
163 452, 477, 478, 486, 498, 501, and 505. Close inspection of these residues shows favorable
164 interactions by residues R452, N477, R498, Y501, and H505 compared to their corresponding ones
165 in the prototype strain. Residues D405 and K478 are somewhat distant from ACE2, while V486
166 appears to weaken the interaction with rat ACE2 compared to F486 in other SARS-CoV-2 viruses
167 (Fig. 3D).
168
169 Taken together, the Alpha, Delta and Omicron variants seem to have enhanced binding to the rat
170 ACE2 compared to the prototype virus.
171
172 **Discussion**
173 Both serological and molecular data from this study suggested the rats from NYC were exposed to
174 SARS-CoV-2. We found that of the tested rats, 16.5% were seropositive and 5.1% were qRT-PCR
175 positive to SARS-CoV-2, which showed a higher exposure frequency than previous reports (11,
176 12). Genomic analyses suggested that the viruses in the rats that we collected were associated
177 with the B lineage virus. We speculate SARS-CoV-2 exposure could have occurred during the early
178 stages of the pandemic when the B lineage virus was predominant in NYC. This is supported by a
179 recent study that reported that the Wuhan-Hu-1-like virus can infect SD rats (16), although an
180 earlier study showed that the prototype Wuhan-Hu-1-like SARS-CoV-2 cannot infect SD rats (6).
181 Such a discrepancy may be due to variation in additional mutations in the challenge Wuhan-Hu-1-
182 like strains or genetic variations in the SD rats used in these studies. Thus, further surveillance is
183 needed to understand the virological prevalence in NYC rats, particularly for several emerging
184 variants with high infectivity among rats, including those that circulated in NYC during the past two
185 years of the COVID-19 pandemic.
186
187 A number of studies suggested that fragments of SARS-CoV-2 genomes were identified in sewage
188 water systems, and that the prevalence of SARS-CoV-2 in sewage water systems coincides with
189 outbreaks in resident human populations (17). However, no evidence has shown that SARS-CoV-

190　2 viruses in sewage water is infectious (18), suggesting that sewage rats may have been exposed
191　to the virus through unknown fomites, e.g. those contaminated with human food wastes. In a recent
192　study, Zeiss et al. (13) showed that, in a controlled laboratory setting studying transmission of
193　another rat respiratory beta coronavirus, SDAV, approximately one-quarter of naïve rats shed virus
194　following fomite exposure. Notably, previously exposed seropositive rats became reinfected with
195　SDAV at similar rates following fomite exposure 114-165 days later, indicating that immunity is
196　temporary. Two of four rats (Rat #2 and #19) in our study were both seropositive and viral RNA-
197　positive, implying that previously exposed seropositive animals may still contract and shed SARS-
198　CoV-2, consistent with lack of sterilizing immunity in humans exposed to SARS-CoV-2 or rats given
199　SDAV. These data imply that rats previously exposed to SARS-CoV-2 can still contribute to
200　propagation of subsequent variants.
201
202　By using animal models, we further demonstrated that, in addition to Alpha and Beta variants
203　reported earlier (6-9), Delta and Omicron variants can also cause robust infections in SD rats. The
204　tested variants caused robust replication in both upper and lower respiratory tracts of rats, although
205　they did not cause any body weight loss or other clinical signs. Of the three testing variants, Delta
206　replicated the most efficiently. The omicron variant showed a lower viral replication than both Alpha
207　and Delta, although the difference did not reach a statistically significant level between Omicron
208　and Alpha. This finding is in line with earlier reports that Omicron replicated less efficiently and
209　caused less lung pathology in wildtype or human ACE2 transgenic mice or hamsters compared
210　with other variants (19, 20).
211
212　Structural modeling showed that all three variants Alpha, Delta and Omicron have enhanced
213　binding to the rat ACE2 compared to the prototype Wuhan-Hu-1-like virus. In light of the
214　biochemical data that Alpha and Delta RBDs bind to rat ACE2 equally well (14), the difference in
215　the replication efficiency of the three viruses could be due to factors other than receptor binding
216　affinity. It is also interesting to note that many RBD mutations observed in the three variants, such
217　as N501Y in Alpha and L452R/T478K in Delta, interact with ACE2 residues that vary between
218　human and rat/mouse (Fig. 4E). Therefore, rats and mouse likely play an important role in the
219　evolution of Alpha, Delta, Omicron variants, as previously proposed by Zhang et al (15).
220
221　In addition to receptor binding, a number of other studies suggested that other structural and non-
222　structural proteins may play a critical role in the viral replication *in vivo* and the host tropism of
223　SARS-CoV-2 viruses. Syed et al. showed that, despite envelope protein substitutions inhibiting
224　virus assembly, Omicron has an overall higher assembly efficiency than the original SARS-CoV-2,
225　similar to Delta variant (21). Bojkova et al. showed that the Omicron variant is less effective in
226　antagonizing the interferon response and has higher sensitivity in interferon treatment than the
227　Delta variant which may be relevant with the substitutions on NSP3, NSP12, NSP13, nucleocapsid,
228　and ORF3 proteins (22, 23). Of interest, Omicron did not have any observed amino acid
229　substitutions throughout the course of virus challenge in SD rats, whereas Alpha and Delta did for
230　spike, nucleoprotein, or non-structural proteins NSP6 and NSP13. The roles of these amino acid
231　substitutions on virus fitness needs to be further studied.
232
233　In summary, we found that the rats in NYC sewage system have been exposed to SARS-CoV-2,
234　and that the Delta and Omicron variants can infect rats in addition to the Alpha and Beta variants.
235　Our findings highlight the potential risk of secondary zoonotic transmission from rats and the need
236　for further monitoring of SARS-CoV-2 in wild rat populations.
237

Materials and Methods

238
239　**Cells.**
240　Vero E6 cells (CRL-1586, American Type Culture Collection [ATCC]) and 293FT/hACE2+TMPRSS
241　(17) were cultured in Dulbecco's Modified Eagle medium (DMEM, Gibco) supplemented with 10%
242　fetal bovine serum (FBS) at 37°C with 5% CO_2. Rat lung epithelial cells L2 (CCL-149, ATCC) were
243　cultured in F-12K Medium (ATCC) supplemented with 10% FBS at 37°C with 5% CO_2. Rat primary

244   tracheal epithelial cells (Cell Biologics) were grown on culture flasks or plates pre-coated with
245   gelatin-based coating solution (Cell Biologics) in Complete Epithelial Cell Medium (Cell Biologics)
246   at 37°C with 5% CO_2.
247

248   **Viruses.**
249   The SARS-CoV-2/USA/CA_CDC_5574/2020 (B.1.1.7, NR-54011, BEI resources), and SARS-
250   CoV-2/human/USA/MD-HP05285/2021 (B.1.617.2, NR-55671, BEI resources) were propagated
251   on Vero E6 cells. The SARS-CoV-2/USA/MO-CV40709/2022 (BA.5.5, GIAID access No.
252   EPI_ISL_15823386) were recovered from human nasopharyngeal swabs and propagated on Vero
253   E6 cells.
254

255   **Virus challenge in rats.**
256   Six-week-old female SAS outbred Sprague Dawley (SD) rats (Charles River Laboratories) were
257   housed in individually ventilated cages. SD rats were anesthetized with isoflurane, followed by
258   intranasal inoculation with 2×10^4 PFU/rat of SARS-CoV-2 diluted in 50 μl PBS. Clinical evaluation
259   was performed daily, and body weight was determined daily through 10 dpi. At 2, 4, and 21 dpi,
260   animals were euthanized for blood and tissue collection for seroconversion evaluation, viral load
261   titration, and histology staining, respectively.
262

263   **Wild rat capture and sample collection.**
264   In the fall of 2021, APHIS Wildlife Services conducted sampling of Norway rats (*Rattus norvegicus*)
265   in New York City (NYC) to look for evidence of SARS-CoV-2 infection. Methodology included
266   trapping and collecting biological samples from rats around wastewater systems. Two trapping
267   efforts during September and November were conducted with permission from the NYC
268   Department of Parks and Recreation. Each effort consisted of three days of pre-baiting followed by
269   four nights of trapping. Most animals were captured in city parks within the borough of Brooklyn,
270   although some were captured near buildings outside of park boundaries. Once the animals were
271   euthanized, biologists collected and processed fresh blood samples. Over the course of eight
272   trapping nights, 79 rats were trapped and sampled. Blood samples along with the carcasses were
273   shipped to the Wildlife Services National Wildlife Disease Program in Fort Collins, Co where tissues
274   were extracted and sent to the University of Missouri for additional testing.

275   **Infectious viral titration by $TCID_{50}$.**
276   Animal tissue were homogenized in DMEM with 0.3% bovine serum albumin (Sigma-Aldrich) and
277   1% penicillin/streptomycin (Gibco, Thermo Fisher Scientific) for 1 min at 6,000 rpm by using a
278   homogenizer (Bertin, Precellys), and debris were pelleted by centrifugation for 10 min at $12,000 \times$
279   *g*. Their infectious virus titers were determined by $TCID_{50}$ with Vero E6 cells.
280

281   **Viral RNA detection.**
282   The RNA was extracted from the tissue homogenates by using GeneJet viral DNA/RNA purification
283   kit (Thermo Fisher) or MagMax Pathogen RNA/DNA Kit (Thermo Fisher). The viral RNA was
284   detected and quantified by qRT-PCR following the SARS-CoV-2 diagnosis panels by N1 (Forward
285   primer sequence: 5'-GAC CCC AAA ATC AGC GAA AT-3', Reverse primer sequence: 5'-TCT GGT
286   TAC TGC CAG TTG AAT CTG-3', Probe sequence: 5'-ACC CCG CAT TAC GTT TGG TGG ACC-
287   3') and/or N2 primer/probe mix (Forward primer sequence: 5'-TTACAAACATTGGCCGCAAA-3',
288   Reverse primer sequence: 5'-GCGCGACATTCCGAAGAA-3', Probe sequence: 5'-
289   ACAATTTGCCCCCAGCGCTTCAG-3'). The RT-qPCR was performed according to the
290   manufacturer's protocol using TaqMan Fast Virus 1-Step Master Mix (Thermo Fisher). Fluorescent
291   signals were acquired using QuantStudio 6 Real-time PCR system (Thermo Fisher).
292

293   **Measurement of cytokine/chemokine expression.**
294   Total RNA was extracted from rat tissues by using a combination method of Trizol (Thermo Fisher
295   Scientific) and RNeasy Mini kit (Qiagen) (24). The genomic DNA was removed by on-column
296   DNase I (Qiagen) treatment during the RNA extraction. The RNA then was reverse transcribed into

297 cDNA with SuperScript III Reverse Transcriptase (Thermo Fisher Scientific) with random hexamer
298 primers (Thermo Fisher Scientific). The cDNA was used in real-time PCR with PowerUp SYBR
299 Green Master Mix (Thermo Fisher Scientific) for specific targets (Table S4). The expression of
300 housekeeping gene GAPDH was used to normalize the amount of RNA isolated from tissues. The
301 $2^{-\Delta\Delta Ct}$ methods were used to compare the differential gene expressions between testing samples.
302 The mean fold change ($2^{-\Delta\Delta Ct}$) values of triplicates and standard deviation are represented.
303
304 **Genome sequencing.**
305 SARS-CoV-2 whole-genome sequencing was performed by using QIAseq DIRECT SARS-CoV-2
306 Kit (QIAGEN). The quality of paired-end reads obtained from MiSeq sequencing was analyzed by
307 using Qiagen CLC Genomics Workbench 22.0.1 and the Identify ARTIC V3 SARS-CoV-2 Low
308 Frequency and Shared Variants (Illumina) workflow was used in genetic variant analyses.
309 Nucleotide sequences were aligned using MAFFT v7.471, and the mutations were analyzed using
310 nextclade (https://clades.nextstrain.org). Pan-viral target hybridization enrichment sequencing was
311 performed by using RNA Prep with Enrichment (L) Tagmentation Kit (Illumina) and Comprehensive
312 Viral Research Panel (Twist Biosciences).

313 **Phylogenetic analyses and molecular characterization.**
314 Time-scaled phylogenetic trees were generated using the two rat samples containing > 10%
315 coverage (Rat# 2 and 19), five reference sequences for each variant of concern (Alpha, Beta, Delta,
316 Gamma, and Omicron), five reference sequences for lineage A and lineage B viruses, and three
317 randomly selected NYC sequences from each month. Phylogenetic analyses were performed using
318 BEAST v2.7.0 with the Hasegawa, Kishino, and Yano (HKY)+$\lceil_4$ substitution model, an exponential
319 coalescent growth prior, and a strict molecular clock. Independent runs were performed with chain
320 lengths of 10,000,000 steps and sampled every 5,000 steps per run with a 10% burn-in. The
321 resulting trees were summarized with TreeAnnotator and visualized using FigTree. A posterior
322 probabilities cutoff of 0.70 was used to assess tree topology.

323 All publicly available sequences and associated metadata used in this dataset are published in
324 GISAID's EpiCoV database. All sequences in this dataset are compared relative to hCoV-
325 19/Wuhan/WIV04/2019 (WIV04), the official reference sequence employed by GISAID
326 (EPI_ISL_402124). Learn more at https://gisaid.org/WIV04. To view the contributors of each
327 individual sequence with details such as accession number, virus name, collection date, originating
328 lab and submitting lab, and the list of authors, please visit the doi listed with each dataset:
329
330 **Data availability for GISAID samples included in our analyses:**
331 GISAID Identifier: EPI_SET_221019xq
332 doi: 10.55876/gis8.221019xq EPI_SET_221019xq is composed of 49 individual genome
333 sequences. The collection dates range from 2019-12-24 to 2021-11-17; Data were
334 collected in 11 countries and territories.
335
336
337 **Virus isolation.**
338 Virus isolation was done on Vero E6 cells, 293FT/hACE2+TMPRSS, L2, or rat primary tracheal
339 epithelial cells. 200 µl of supernatant from homogenized tissues were mixed with an equal volume
340 of cell culture medium and then inoculated onto pre-seeded cells in 6-well plates. After 1 hour of
341 adsorption, the inoculum was removed, and the cells were washed with PBS and covered with
342 fresh cell culture medium. The cells were monitored daily for cytopathogenic effects (CPE) and the
343 supernatants were harvested at 3~5 dpi. The supernatants were inoculated to fresh cells for a
344 maximum of 3 times until CPE was observed. The supernatants from the last inoculation were
345 subjected to viral RNA extraction and SARS-CoV-2 specific real-time RT-PCR using SARS-CoV-2
346 diagnosis panels.
347

ELISA.
Anti-SARS-CoV-2 spike and anti-SARS-CoV-2 receptor binding domain (RBD) IgG or IgM antibodies were determined by using stabilized spike protein (NR-53524, BEI resources) or RBD (NR-53366, BEI resources) of SARS-CoV-2, respectively. The proteins were coated to 96-well ELISA plates (Nunc-Immuno, Thermo Scientific) at a concentration of 1 µg/ml in PBS. The plates were then blocked with 100 µl of 1% Bovine Serum Albumin (BSA, Research Products International) buffered in PBS containing 0.1% Tween 20 (PBST) and incubated at room temperature for 1 h. 1:100 diluted rat serum samples were added to the plates for 1 h incubation at 37 °C. After extensive washing with PBST, horseradish peroxidase (HRP)-conjugated goat anti-rat IgG (1:8,000, Thermo Scientific) or anti-rat IgM (1:8,000, Thermo Scientific) was added for 1 h at 37 °C. Following five-time washes with PBST, 100 µL of TMB-ELISA substrate (1-Step; Thermo Fisher Scientific) was added into each well. After 15 min incubation, the reaction was stopped by adding 100 µL of 1 M H_2SO_4 solution and optical densities were read at 450 nm (OD450) using Cytation 5 Cell Imaging Multimode Reader (Bio-Tek Instruments). Cutoff value was determined based on the mean background reactivity of all serum samples from naïve SD rats multiplied by 3.

Microneutralization assay.
The serum samples were heat-inactivated at 56 °C for 1 hour and then were two-fold serially diluted with a starting dilution of 1:5. The serum dilutions were mixed with equal volumes of 100 $TCID_{50}$ of SARS-CoV-2 as indicated. After 1 h of incubation at 37 °C, 3.5×10^4 Vero E6 cells were added into the serum-virus mixture in 96-well plates. The plates were incubated for 2 days at 37 °C in 5% CO2 and then the cells were fixed in 10% paraformaldehyde, penetrated by 0.1% TritonX-100, and strained with monoclonal rabbit antibody against SARS-CoV-2 nucleocapsid (Sino Biological). This was subsequently detected by the addition of HRP-conjugated goat anti-rabbit IgG (Thermo Fisher Scientific) and TMB-ELISA substrate (Thermo Fisher Scientific). OD_{450} was measured by Cytation 5 (Bio-Tek). The serum neutralizing titer is the reciprocal of the highest dilution resulting in an infection reduction of >50%.

Structure modeling.
The tertiary structure of the rat ACE2 (NP_001012006.1) was predicted by Alphafold2 using the Google colab server (https://colab.research.google.com/) (25). The RBD structure of alpha (SARS-CoV-2/USA/CA_CDC_5574/2020, B.1.1.7), delta (SARS-CoV-2/human/USA/MD-HP05285/2021, B.1.617.2) and omicron (SARS-CoV-2/USA/MO-CV40709/2022, BA.5.5) was taken from the PDB ID 7FBK, 7URQ, and 7XWA, respectively. To model the rat ACE2:RBD complex structure, rat ACE2 structural model and the structure of each of the three RDB domains were superposed onto their respective homologs in PDB ID 7XO9, the SARS-CoV-2 Omicron BA.2 variant RBD complexed with human ACE2 (26) using Pymol (The PyMOL Molecular Graphics System, Version 2.0 Schrödinger, LLC). The resulting complex structures were subjected to energy minimization using Phenix (27). Structure figures were prepared using Pymol.

Statistical analysis.
Statistical significance was tested using a one-way ANOVA with Tukey's multiple comparisons by Graphpad Prism 9.1.0.

Ethics statement.
Rats were captured in Brooklyn under a wildlife damage management agreement between USDA/APHIS Wildlife Services and the New York City Department of Parks and Recreation. The animal experiments were performed under the protocol number #38742 approved by the Care and Use of Laboratory Animals of the University of Missouri per the USDA Animal Welfare Regulations. All experiments involved with live viruses were performed in an approved biosafety level 3 (BSL-3) or animal biosafety level 3 (ABSL-3) facility at the Laboratory of Infectious Diseases, University of Missouri-Columbia under protocol #20-14 in compliance with the Institutional Biosafety Committee of the University of Missouri-Columbia.

10

Acknowledgments

References

1. Medicine JHUo. 2022. Coronavirus Resource Center. https://coronavirus.jhu.edu/data. Accessed March 4.

2. Cui S, Liu Y, Zhao J, Peng X, Lu G, Shi W, Pan Y, Zhang D, Yang P, Wang Q. 2022. An Updated Review on SARS-CoV-2 Infection in Animals. Viruses 14.

3. Chandler JC, Bevins SN, Ellis JW, Linder TJ, Tell RM, Jenkins-Moore M, Root JJ, Lenoch JB, Robbe-Austerman S, DeLiberto TJ, Gidlewski T, Kim Torchetti M, Shriner SA. 2021. SARS-CoV-2 exposure in wild white-tailed deer (Odocoileus virginianus). Proc Natl Acad Sci U S A 118.

4. Hale VL, Dennis PM, McBride DS, Nolting JM, Madden C, Huey D, Ehrlich M, Grieser J, Winston J, Lombardi D, Gibson S, Saif L, Killian ML, Lantz K, Tell RM, Torchetti M, Robbe-Austerman S, Nelson MI, Faith SA, Bowman AS. 2022. SARS-CoV-2 infection in free-ranging white-tailed deer. Nature 602:481-486.

5. Hammer AS, Quaade ML, Rasmussen TB, Fonager J, Rasmussen M, Mundbjerg K, Lohse L, Strandbygaard B, Jorgensen CS, Alfaro-Nunez A, Rosenstierne MW, Boklund A, Halasa T, Fomsgaard A, Belsham GJ, Botner A. 2021. SARS-CoV-2 Transmission between Mink (Neovison vison) and Humans, Denmark. Emerg Infect Dis 27:547-551.

6. Shuai H, Chan JF, Yuen TT, Yoon C, Hu JC, Wen L, Hu B, Yang D, Wang Y, Hou Y, Huang X, Chai Y, Chan CC, Poon VK, Lu L, Zhang RQ, Chan WM, Ip JD, Chu AW, Hu YF, Cai JP, Chan KH, Zhou J, Sridhar S, Zhang BZ, Yuan S, Zhang AJ, Huang JD, To KK, Yuen KY, Chu H. 2021. Emerging SARS-CoV-2 variants expand species tropism to murines. EBioMedicine 73:103643.

7. Pan T, Chen R, He X, Yuan Y, Deng X, Li R, Yan H, Yan S, Liu J, Zhang Y, Zhang X, Yu F, Zhou M, Ke C, Ma X, Zhang H. 2021. Infection of wild-type mice by SARS-CoV-2 B.1.351 variant indicates a possible novel cross-species transmission route. Signal Transduct Target Ther 6:420.

8. Zhang C, Cui H, Li E, Guo Z, Wang T, Yan F, Liu L, Li Y, Chen D, Meng K, Li N, Qin C, Liu J, Gao Y, Zhang C. 2022. The SARS-CoV-2 B.1.351 Variant Can Transmit in Rats But Not in Mice. Front Immunol 13:869809.

9. Montagutelli X, Prot M, Levillayer L, Salazar EB, Jouvion G, Conquet L, Beretta M, Donati F, Albert M, Gambaro FJB. 2021. Variants with the N501Y mutation extend SARS-CoV-2 host range to mice, with contact transmission. BioRxiv.

10. Bosco-Lauth AM, Root JJ, Porter SM, Walker AE, Guilbert L, Hawvermale D, Pepper A, Maison RM, Hartwig AE, Gordy P, Bielefeldt-Ohmann H, Bowen RA. Survey of peridomestic mammal susceptibility to SARS-CoV-2 infection. doi:https://doi.org/10.1101/2021.01.21.427629.

11. Miot EF, Worthington BM, Ng KH, de Lataillade LG, Pierce MP, Liao Y, Ko R, Shum MH, Cheung WY, Holmes EC, Leung KS, Zhu H, Poon LL, Peiris MJ, Guan Y, Leung GM, Wu

453   JT, Lam TT. 2022. Surveillance of Rodent Pests for SARS-CoV-2 and Other
454   Coronaviruses, Hong Kong. Emerg Infect Dis 28:467-470.
455   12.   Colombo VC, Sluydts V, Marien J, Vanden Broecke B, Van Houtte N, Leirs W, Jacobs L,
456   Iserbyt A, Hubert M, Heyndrickx L, Goris H, Delputte P, De Roeck N, Elst J, Arien KK,
457   Leirs H, Gryseels S. 2022. SARS-CoV-2 surveillance in Norway rats (Rattus norvegicus)
458   from Antwerp sewer system, Belgium. Transbound Emerg Dis 69:3016-3021.
459   13.   Zeiss CJ, Asher JL, Vander Wyk B, Allore HG, Compton SR. 2021. Modeling SARS-CoV-
460   2 propagation using rat coronavirus-associated shedding and transmission. PLoS One
461   16:e0260038.
462   14.   Yao W, Ma D, Wang H, Tang X, Du C, Pan H, Li C, Lin H, Farzan M, Zhao J, Li Y, Zhong
463   G. 2021. Effect of SARS-CoV-2 spike mutations on animal ACE2 usage and in vitro
464   neutralization sensitivity.
465   https://wwwbiorxivorg/content/101101/20210127428353v3fullpdf.
466   15.   Zhang W, Shi K, Geng Q, Ye G, Aihara H, Li F. 2022. Structural basis for mouse receptor
467   recognition by SARS-CoV-2 omicron variant. Proc Natl Acad Sci U S A
468   119:e2206509119.
469   16.   Yu D, Long Y, Xu L, Han JB, Xi J, Xu J, Yang LX, Feng XL, Zou QC, Qu W, Lin J, Li MH,
470   Yao YG. 2022. Infectivity of SARS-CoV-2 and protection against reinfection in rats. Zool
471   Res 43:945-948.
472   17.   Smyth DS, Trujillo M, Gregory DA, Cheung K, Gao A, Graham M, Guan Y,
473   Guldenpfennig C, Hoxie I, Kannoly S, Kubota N, Lyddon TD, Markman M, Rushford C,
474   San KM, Sompanya G, Spagnolo F, Suarez R, Teixeiro E, Daniels M, Johnson MC,
475   Dennehy JJ. 2022. Tracking cryptic SARS-CoV-2 lineages detected in NYC wastewater.
476   Nat Commun 13:635.
477   18.   Robinson CA, Hsieh HY, Hsu SY, Wang Y, Salcedo BT, Belenchia A, Klutts J, Zemmer
478   S, Reynolds M, Semkiw E, Foley T, Wan X, Wieberg CG, Wenzel J, Lin CH, Johnson
479   MC. 2022. Defining biological and biophysical properties of SARS-CoV-2 genetic material
480   in wastewater. Sci Total Environ 807:150786.
481   19.   Halfmann PJ, Iida S, Iwatsuki-Horimoto K, Maemura T, Kiso M, Scheaffer SM, Darling
482   TL, Joshi A, Loeber S, Singh G, Foster SL, Ying B, Case JB, Chong Z, Whitener B,
483   Moliva J, Floyd K, Ujie M, Nakajima N, Ito M, Wright R, Uraki R, Warang P, Gagne M, Li
484   R, Sakai-Tagawa Y, Liu Y, Larson D, Osorio JE, Hernandez-Ortiz JP, Henry AR,
485   Ciuoderis K, Florek KR, Patel M, Odle A, Wong LR, Bateman AC, Wang Z, Edara VV,
486   Chong Z, Franks J, Jeevan T, Fabrizio T, DeBeauchamp J, Kercher L, Seiler P,
487   Gonzalez-Reiche AS, Sordillo EM, Chang LA, van Bakel H, et al. 2022. SARS-CoV-2
488   Omicron virus causes attenuated disease in mice and hamsters. Nature 603:687-692.
489   20.   Yuan S, Ye ZW, Liang R, Tang K, Zhang AJ, Lu G, Ong CP, Man Poon VK, Chan CC,
490   Mok BW, Qin Z, Xie Y, Chu AW, Chan WM, Ip JD, Sun H, Tsang JO, Yuen TT, Chik KK,
491   Chan CC, Cai JP, Luo C, Lu L, Yip CC, Chu H, To KK, Chen H, Jin DY, Yuen KY, Chan
492   JF. 2022. Pathogenicity, transmissibility, and fitness of SARS-CoV-2 Omicron in Syrian
493   hamsters. Science 377:428-433.
494   21.   Syed AM, Ciling A, Taha TY, Chen IP, Khalid MM, Sreekumar B, Chen PY, Kumar GR,
495   Suryawanshi R, Silva I, Milbes B, Kojima N, Hess V, Shacreaw M, Lopez L, Brobeck M,
496   Turner F, Spraggon L, Tabata T, Ott M, Doudna JA. 2022. Omicron mutations enhance
497   infectivity and reduce antibody neutralization of SARS-CoV-2 virus-like particles. Proc
498   Natl Acad Sci U S A 119:e2200592119.
499   22.   Bojkova D, Widera M, Ciesek S, Wass MN, Michaelis M, Cinatl J, Jr. 2022. Reduced
500   interferon antagonism but similar drug sensitivity in Omicron variant compared to Delta
501   variant of SARS-CoV-2 isolates. Cell Res 32:319-321.
502   23.   Bojkova D, Rothenburger T, Ciesek S, Wass MN, Michaelis M, Cinatl J, Jr. 2022. SARS-
503   CoV-2 Omicron variant virus isolates are highly sensitive to interferon treatment. Cell
504   Discov 8:42.
505   24.   Untergasser A. 2008. RNAprep - Trizol combined with Columns.
506   http://www.molbi.de/protocols/rna_prep_comb_trizol_v1_0.htm. Accessed April 13.

507 25. Mirdita M, Schutze K, Moriwaki Y, Heo L, Ovchinnikov S, Steinegger M. 2022. ColabFold:
508   making protein folding accessible to all. Nat Methods 19:679-682.
509 26. Xu Y, Wu C, Cao X, Gu C, Liu H, Jiang M, Wang X, Yuan Q, Wu K, Liu J, Wang D, He X,
510   Wang X, Deng SJ, Xu HE, Yin W. 2022. Structural and biochemical mechanism for
511   increased infectivity and immune evasion of Omicron BA.2 variant compared to BA.1 and
512   their possible mouse origins. Cell Res 32:609-620.
513 27. Liebschner D, Afonine PV, Baker ML, Bunkoczi G, Chen VB, Croll TI, Hintze B, Hung
514   LW, Jain S, McCoy AJ, Moriarty NW, Oeffner RD, Poon BK, Prisant MG, Read RJ,
515   Richardson JS, Richardson DC, Sammito MD, Sobolev OV, Stockwell DH, Terwilliger TC,
516   Urzhumtsev AG, Videau LL, Williams CJ, Adams PD. 2019. Macromolecular structure
517   determination using X-rays, neutrons and electrons: recent developments in Phenix. Acta
518   Crystallogr D Struct Biol 75:861-877.

519
520
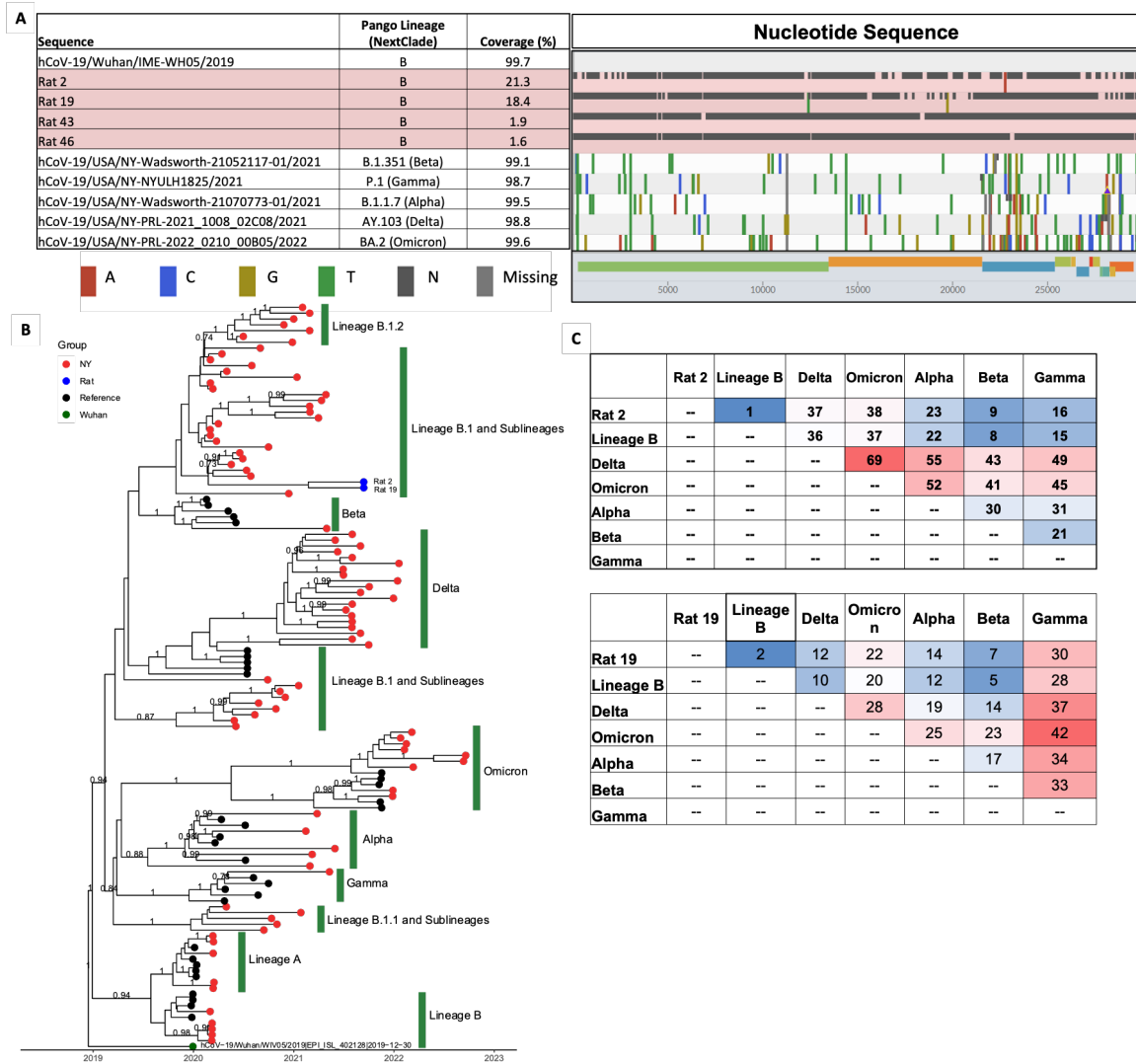
Figure 1. SARS-CoV-2 genomic sequencing in wild rats. (A) SARS-CoV-2 genomes found in rats in comparison with reference wild-type virus and variants of concern. Analyses were performed and visualized using https://clades.nextstrain.org. Reference sequences were downloaded from GISAID. (B) Phylogenetic tree of rat SARS-CoV-2 sequences with reference sequences from wild-type viruses and variants of concern. Branches with posterior probability ≥ 0.7 are labeled. (C) Distance matrices of regions covered by each rat-derived SARS-CoV-2 genome. Lineage B is represented by hCoV-19/Wuhan/IME-WH05/2019|EPI_ISL_529217|2019-12-30, Delta by hCoV-19/USA/NY-Wadsworth-21052117-01/2021|EPI_ISL_2278740|2021-05-01, Omicron by hCoV-19/USA/NY-NYULH1825/2021|EPI_ISL_2427410|2021-05-11, Alpha by hCoV-19/USA/NY-Wadsworth-21070773-01/2021|EPI_ISL_2868594|2021-05-31, Beta by hCoV-19/USA/NY-PRL-2021_1008_02C08/2021|EPI_ISL_5285364|2021-10-03.

537
538
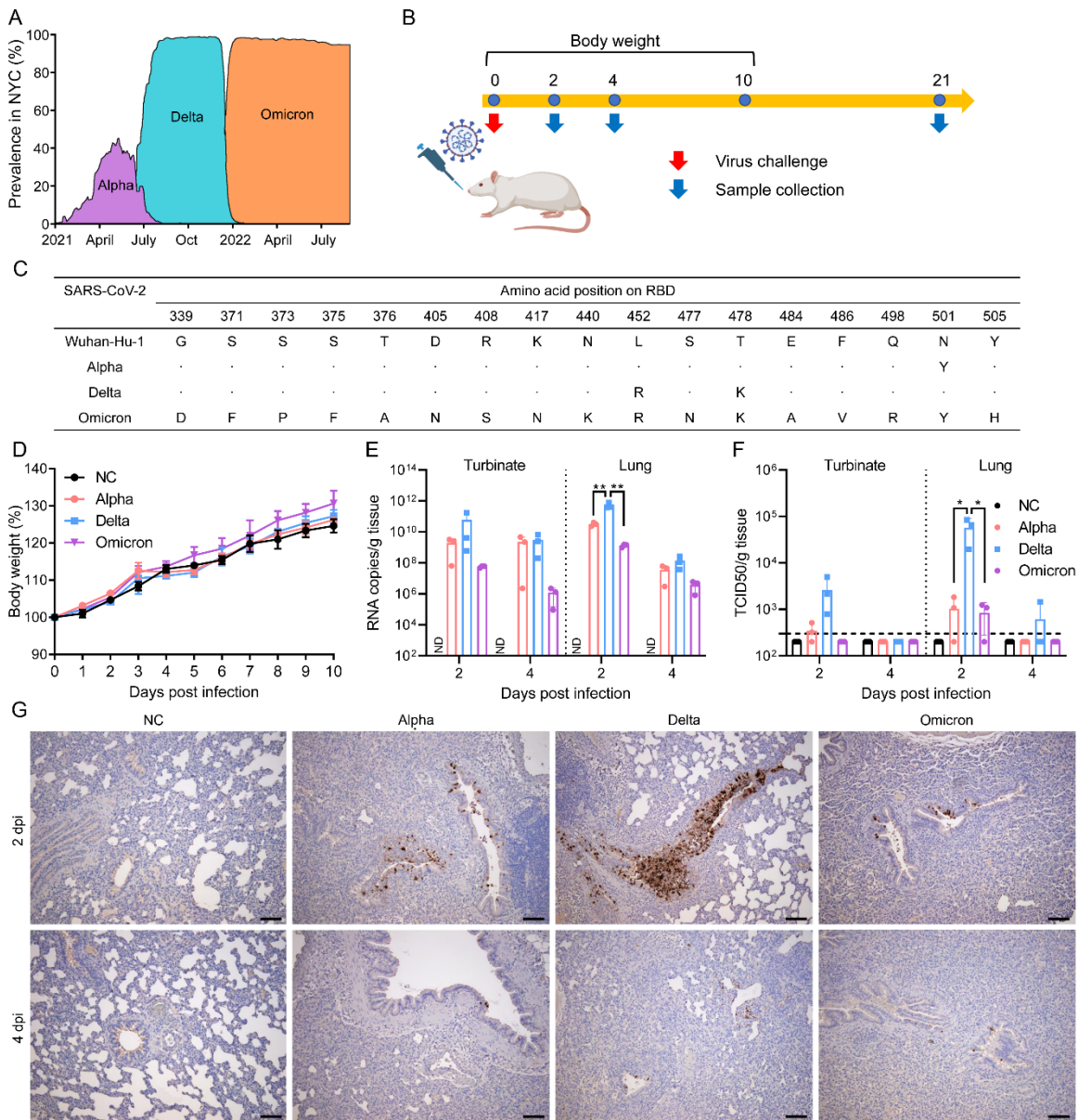
539
540

Figure 2. SD rats are susceptible to infection of Alpha, Delta, and Omicron variants. (A) The prevalence of Alpha, Delta, and Omicron variants in NYC. The figure was adapted from https://outbreak.info. (B) Scheme of the virus challenge experiment using 6-week-old SD rats. (C) Amino acid changes of Alpha, Delta, and Omicron variants across RBD compared to Wuhan-Hu-1 (NCBI access No.: MN908947.3). (D) Body weight of rats mock infected or infected with either Alpha, Delta, or Omicron variant, Viral RNA copies (E) and infectious viral titers (F) in the turbinate and lungs from rats infected with either Alpha, Delta, or Omicron variant at 2 or 4 dpi. *, $p < 0.05$; **, $p < 0.01$. (G) Detection of SARS-CoV-2 nucleocapsid protein at bronchial epithelial cells by immunohistochemistry at 2 and 4 dpi. Scale bar, 100 μm.

550
551
552

15
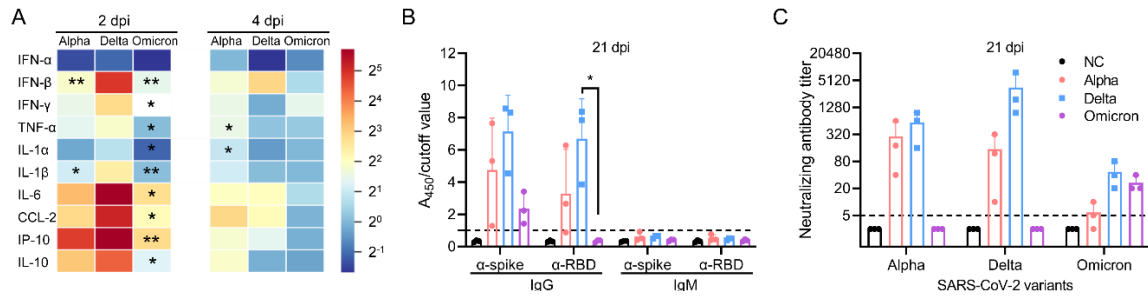
553
554
Figure 3. Innate and adapted immune responses induced by SARS-CoV-2 infection in SD rats. (A) Pro-inflammatory cytokine/chemokine expression in lungs from rats infected with either Alpha, Delta, or Omicron variant. Asterisks indicate the significant difference between the indicated variant and Delta. *, $p < 0.05$; **, $p < 0.01$. (B) Wuhan-Hu-1 spike protein or RBD specific IgG or IgM antibody titers. A_{450}/Cutoff was interpreted as negative if $\leqslant 1.0$, and seropositive if >1.0. The cutoff value was 3-fold of mean of negative serum samples. (C) Alpha, Delta, or Omicron specific neutralizing antibody titers induced by mock-infected rats or rats infected with either Alpha, Delta, or Omicron variant.

563
564

565
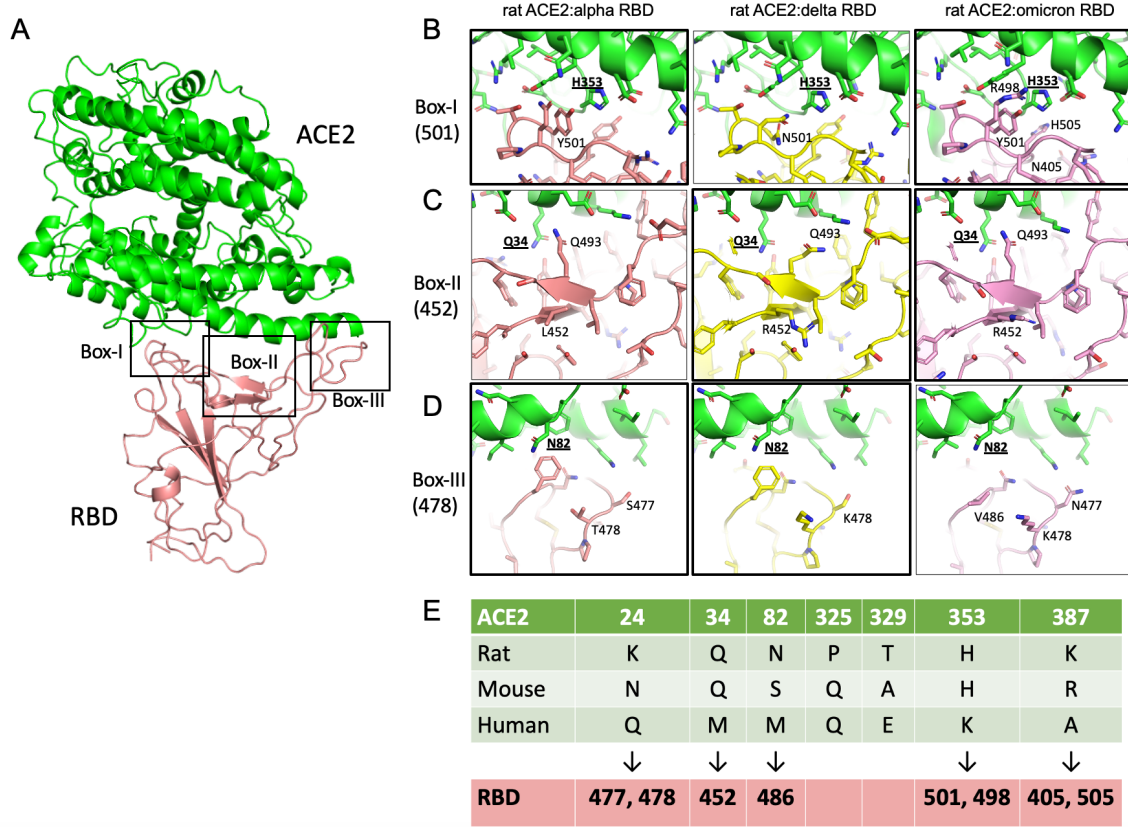
Figure 4. Interactions between the receptor binding domain (RBD) of SARS-CoV-2 variants Alpha, Delta, and Omicron and the rat ACE2. (A) Rat ACE2 in complex with RBD. The three major contact sites in box-1, box-2 and box-3 are shown in subpanels B, C, and D, respectively. Interactions mediated by alpha, delta and omicron RBDs are compared side-by-side. Black thick outlines highlighted favorable interactions. (E) A list of ACE2 amino acid variations between rat, mouse and human at the RBD interface. Many RBD mutations in alpha, delta and omicron variants are located near host-specfic ACE2 residues, as indicated by black arrows.

576 **Tables**

577
578 **Table 1.** Information on rats collected in Brooklyn of NYC with conclusive seropositive or qRT-
579 PCR positive samples
580

Category	Rat code	Collection date	ELISA A$_{450}$/Cutoff[a]				qRT-PCR[b]	
			IgG against spike	IgG against RBD	IgM against spike	IgM against RBD	N1	N2
Seropositive	#4	Sep 13	1.046	1.001	0.459	0.772	n.d.	38.42
	#40	Sep 16	1.216	1.132	0.591	0.790	n.d.	n.d.
	#42	Sep 16	1.222	1.049	0.583	0.683	n.d.	n.d.
	#56	Nov 14	1.397	1.538	0.739	0.629	n.d.	n.d.
	#59	Nov 14	1.036	1.071	0.550	0.355	n.d.	n.d.
	#64	Nov 15	1.016	1.199	0.614	0.587	n.d.	n.d.
	#65	Nov 15	1.163	1.021	1.889	0.591	n.d.	n.d.
	#20	Sep 13	1.199	0.906	1.554	1.314	n.d.	n.d.
	#24	Sep 14	0.925	0.721	1.857	1.172	n.d.	n.d.
	#48	Nov 14	0.308	0.293	1.419	1.373	n.d.	n.d.
	#79	Nov 16	0.787	0.731	1.174	1.047	n.d.	n.d.
qRT-PCR positive	#2	Sep 13	0.238	0.207	0.552	1.063	33.95	34.61
	#43	Sep 16	0.573	0.481	0.296	0.323	32.27	34.28
Both seropositive and qRT-PCR positive	#19	Sep 13	1.001	1.000	0.480	0.569	36.36	35.83
	#46	Sep 16	1.104	1.144	0.587	0.850	35.23	37.31

581 [a], A$_{450}$/Cutoff was interpreted as negative if $\leq$ 1.0, and seropositive if >1.0. The cutoff value was
582 3-fold of mean of negative serum samples. Triplicate was conducted and the mean was shown.
583 [b], Ct value was interpreted as positive if <40. Triplicate was conducted and the mean was shown.
584 n.d., undetectable.
585
586

18